PCCP

Accepted Manuscript

ROYAL SOCIETY OF CHEMISTRY

www.rsc.org/pccp

Journal Name

ARTICLE

Nonlinear optical chromophores based on Dewar's Rules: Enhancement of electro-optic activity by introducing heteroatoms to the donor or bridge

Received 00th January 20xx,
Accepted 00th January 20xx

DOI: 10.1039/x0xx00000x

www.rsc.org/

Huajun Xu[ac], Dan Yang[ac], Fenggang Liu[ac], Mingkai Fu[bc], Shuhui Bo[a*], Xinhou Liu[a*] and Yuan Cao[ad].

In this work, we investigated the enhancement of the electro-optic response by introducing electron-rich heteroatoms as additional donors to the donor or bridge of conventional second-order nonlinear optical chromophore. A series of chromophores **C2**-**C4** based on the same tricyanofuran acceptor(TCF) but with different heteroatoms in the alkylamino phenyl donor(**C2** or **C3**) or thiophene bridge (**C4**) have been synthesized andsystematically investigated. Density functional theory calculations suggested that chromophore **C2**-**C4** had smaller energy gap and larger first-order hyperpolarizability (β) than traditional chromophore **C1** due to the additional heteroatoms. Single crystal structure analyses and optimized configurations indicate rational introduced heteroatom group would bring larger β and weaker intermolecular interactions which were beneficial to translate molecular β into macro electro-optic activity in electric field poled films. The electro-optic coefficient of poled films containing 25 wt% of these new chromophores doped in amorphous poly-carbonate afforded values of 83 and 91 pm V^{-1} at 1310 nm for chromophores **C3** and **C4**,respectively, which is two times higher than that of the traditional chromophore **C1** (39 pm/V). High r_{33} values indicated that introducing heteroatom to the to the donor and bridge of conventional molecular can efficiently improve the electron-donating ability, which improves the β. The long-chain on the donor or bridge part, acting as the isolation group, may reduce inter-molecular electrostatic interactions, thus enhancing the macroscopic EO activity. These results, together with good solubility and compatibility with polymer, show the new chromophore's potential application in electro-optic device.

Introduction

During recent decades, organic and polymeric electro-optic (EO) materials have drawn much attention due to their attractive potential applications in high speed EO devices with broad bandwidth and low driving voltage.[1] Compared with traditional inorganic and semiconductor materials, the organic EO materials have many advantages such as larger nonlinear optical coefficients, simpler preparation and lower cost.[2-6] As the core component of EO materials, the design and preparation of NLO chromophores have been turned into a hot research spot in the area of organic EO materials.[7-11] To realize application of devices, NLO chromophores should be required to possess several properties: large first-order hyperpolarizability (β), low optical loss at operation wavelength, thermal stability and long-term stability of polar order. Therefore, much great efforts have been paid to the rational design of chromophores with not only high first-order hyperpolarizability but also good thermal and photochemical stabilities, and in addition, good solubility and compatibility with polymer matrix.[12-15]

It is a well-established fact that the conjugation length and donor/acceptor strength of these D-π-A type push-pull chromophore molecules can cause dramatic influences to their second order nonlinear responses.[16, 17] A majority of high performance NLO chromophores up to now can be divided into three blocks: electro-donor (typical alkyl aniline), pi-bridge (isophorone or heterocyclic rings) and strong electro-acceptor. In order to achieve high EO activity, rational design and synthesis of dipolar NLO chromophores with high molecular first hyperpolarizability (β) and robust thermal stability still represents one of the most critical challenges.[18-20] In the past decades, the researches on NLO chromophores have mainly focused on the design of electron bridges and electron acceptors.[17, 21, 22] The electron donors have received much less attention as the general class of traditional alkyl and aryl amines were considered to be the idea electron donors and were constantly-used. There were some systematic works concentrating on researching the substitutions in the π-framework from theoretical and practical domains.[23-27] Jen's group introduced alkylthiol group into the electron-bridge of CLD-type chromophore, which achieved excellent

[a] a.Key Laboratory of Photochemical Conversion and Optoelectronic Materials, Technical Institute of Physics and Chemistry, Chinese Academy of Sciences, Beijing 100190, PR China. E-mail address: boshuhui@mail.ipc.ac.cn, xhliu@mail.ipc.ac.cn and xinhouliu@foxmail.com. Tel.: +86-01-82543528; Fax: +86-01-62554670.
[b] b.Beijing National Laboratory for Molecular Sciences, Institute of Chemistry, Chinese Academy of Sciences, Beijing 100190, PR China.
[c] c.University of Chinese Academy of Sciences, Beijing, 100043, PR China.
[d] College of Chemical Engineering, Sichuan University, Chengdu, 610065, PR China.
† CCDC reference number 1401496.

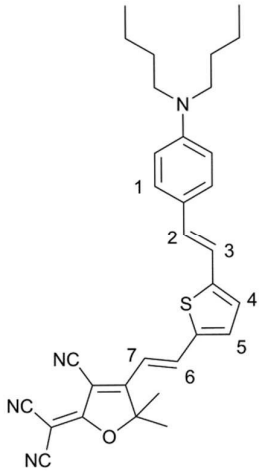

Fig 1. Depiction the substitution positions on the conjugated backbone for FTC-type chromophore.

photostability and large optical nonlinearity. Dalton' group synthesized a series of chromophores based on Bis-(4-methoxyphenyl)hetero-aryl-amino type donors. The chromophores' first-order hyperpolarizabilities and materials' electro optical performance were enhanced effectively. Introducing additional amino group into the donor moiety could effectively modulate the conjugation of the π-electron networks and the electronic character of the charge transfer kinetics, which was proved by simulated calculation.[11, 23, 27-29] As a classical theories, Dewar's rules,[30] have been widely applied into chromophore structure design to increasing nonlinear optical activity and stability.[31, 32] On the basis of this theory, a donor-bridge-acceptor push-pull type nonlinear optical chromophore shows alternating electronegativities along the charge-transfer direction (fig 1). It can be used to predict the change of molecular orbital level. For instance, the energy level of the highest occupied molecular orbital (HOMO) will increase if introducing an electron-donating group into 3, 4, 7 position. At the same time, bathochromic shift of the UV-Vis absorption spectra will be found. In order to systematically investigate the influence of additional heteroatom groups introduced into traditional aniline donor and bridge moieties to first-order hyperpolarizability and macroscopic EO activities, we designed and synthesized chromophores **C2**-**C4**, and measured their physical and chemical properties with care. Chromophores **C1** was used as bench chromophores. Four chromphores' structures showed in Chart 1. For reasonable comparison, these NLO chromophores all choose 2-dicyanomethylene-3-cyano-4,5,5-dimethyl-2,5-dihydrofuran (TCF) as electron acceptors. ^{1}H and ^{13}C NMR, MALDI-TOF and crystal structure analysis were carried out to demonstrate the preparation of these chromophores. Thermal stability, photophysical properties, density functional theory (DFT) calculations and EO activities of these chromophores were systematically studied and compared to illustrate the influences of different heteroatom groups and site on rational NLO chromophore designs.

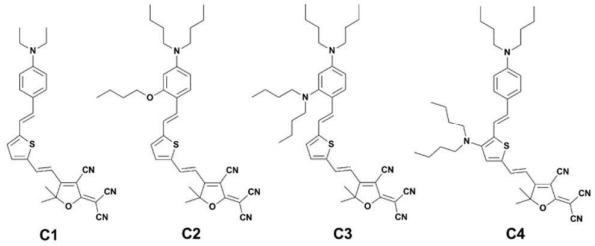

Chart 1. The structures of chromophores **C2**-**C4**.

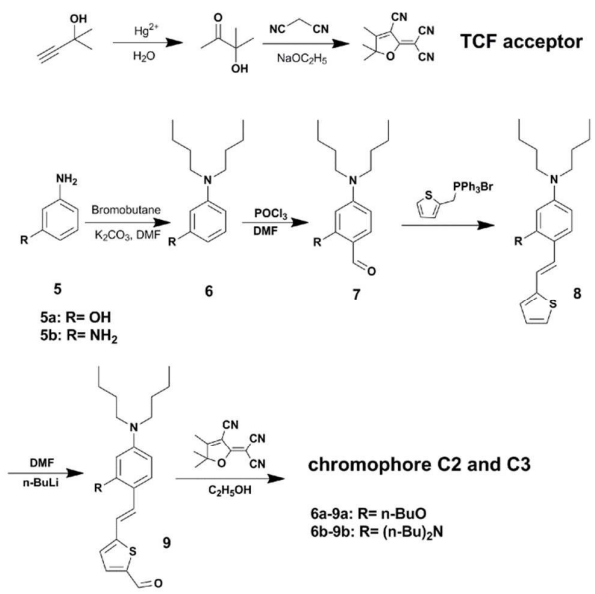

Scheme 1. Synthesis route for **C2**-**C4**.

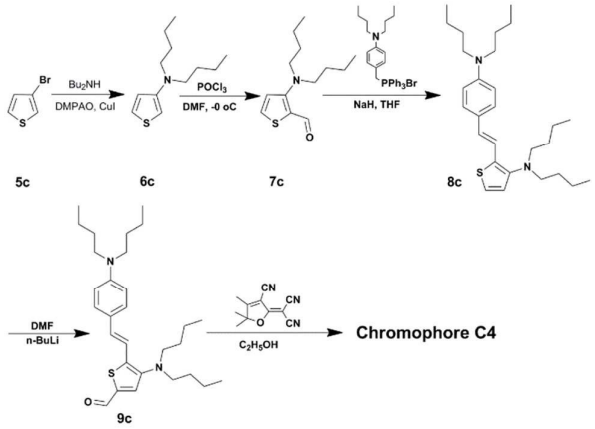

Scheme 2. Synthesis route for **C4**.

Results and discussion

2.1 synthesis and characterization

Synthetic approaches for the chromophores **C2**-**C4** were showed in Scheme 1 and Scheme 2. All reactions were performed under nitrogen protection. TCF acceptor was

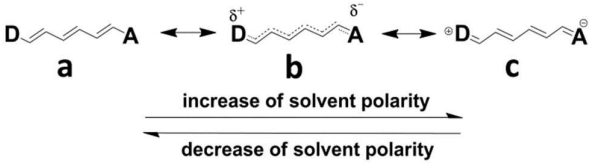

Fig. 2 The schematic representation of electronic transitions for D-π-A system as a function of dielectric media strength.

prepared according to the literature.[33] Chromophores **C2**-**C4** were synthesized in good overall yields through simple routes which have been established for the high yield synthesis of this kind of NLO chromophores.[34, 35] All the chromophores were completely characterized by ^{1}H-NMR, ^{13}C-NMR, MS, UV-Vis spectroscopic analysis and the data obtained were in full agreement with the proposed formulations. The information of crystal structure for chromophore **C3** has been obtained by Single-Crystal X-ray diffraction, which further demonstrated the successful preparation of chromophores.

2.2. Optical properties.

The nature of the CT band and solvatochromic behavior of **C2**-**C4** were investigated using UV-Vis absorption measurements in aprotic solvents with different polarities. The shape and position of the CT band of this type of chromophore mainly depends on the dielectric propertied of the solvents. There are three major electronic structures which have been predicted and illustrated in Fig 3. Generally, the initial increase of the solvent polarity will results in red-shift of absorption maximum for a dye in the neutral ground state due to the strong electron polarization along the conjugated system. This change happens to a certain point, where the electronic structure of the chromophore reaches a cyanine-limit structure.[16, 36-39] Blue-shift of absorption maximum will be observed when further increase of solvent polarity. As discussed in the previous section, their modification by changing the length and chemical composition has a significant effect on the molecular hyperpolarizibility of the molecule. The theory of Bond length alternation (BLA) has furthered the realization of the structure-property relationships within polyene molecules and the use of optimal donor and acceptor strengths for a given bridge. BLA parameter is defined as the average difference in length between adjacent carbon-carbon bonds of a molecule. BLA theory indicates that increasing the values of donor and acceptor strength will improve the proportion of structure **c** (Fig 2) in among three resonance states within certain limits, then BLA parameter will decrease and molecular NLO activity will be enhanced. UV-Vis spectra and solvatochromic data can reveal the change of BLA parameters to some degree. The Fig 3 displays the spectra of **C2**-**C4** in five solvents with different dielectric constants and the spectra data are summarized in Table 1. The positions of λ_{max} for the chromophores prepared in chloroform follow Dewar's rules, which showed large red-shifts. Compared with **C1** (λ_{max}=676 nm), the λ_{max} of chromophore **C2**-**C4** were shifted to the longer wavelength of 719 nm, 734 and 744 nm respectively, which should be attributed to the enhanced electron-donation ability of

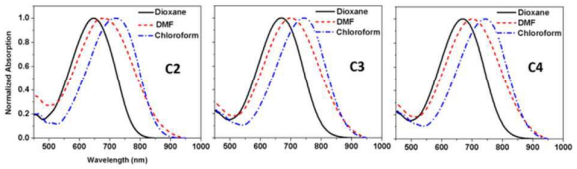

Fig 3. UV-Vis spectra in different solvents.

Table 1. UV-Vis absorption and solvatochromic data of the chromophores

	$\lambda_{max}{}^{a}$/ nm	$\lambda_{max}{}^{b}$/ nm	$\lambda_{max}{}^{c}$/ nm	$\lambda_{max}{}^{d}$/ nm	r_{33}/pm•V^{-1}
C1	621	676	650	638	39
C2	646	719	679	665	68
C3	647	734	665	685	83
C4	669	744	700	694	91

$^{a}\lambda_{max}$, $^{b}\lambda_{max}$, $^{c}\lambda_{max}$ and $^{c}\lambda_{max}$ were measured in dioxane, chloroform, DMF and APC.

additional heteroatom groups conjugated with the π-system. At the same time, because of the fact that nitrogen atom conjugated with the π-system better than oxygen atom, chromophore **C3** showed longer red-shift compared with **C2**. The different sites for heteroatom groups also brought different influences to the maximum absorption wavelength, which we can observe from the spectra of **C3** and **C4** (λ_{max}=734nm, 744nm). The solvatochromic behavior was also explored to investigate the polarity of chromophores. When increasing the solvent dielectric constant from dioxane to chloroform, all of the chromophores showed solvatochromic red-shifts. Chromophores **C2** and **C4** showed similar bathochromic shifts of 73 nm and 75 nm when solvent was changed from dioxane to chloroform, respectively, whereas 44 nm and 40 nm blue-shifts from chloroform to DMF. Chromophores **C2-4** exhibited larger red-shifts and blue-shifts in comparison to chromophores **C1**. It indicated that the π-electrons in there three chromophores are easier to polarized than chromophores **C1**. In three resonance states, structure **c** will contain more proportion for chromophores **C2-4**, which generally mean larger molecular first-order hyperpolarizabilities.

2.3 Theoretical calculations

Theoretical estimation of molecular hyperpolarizability is now a reliable and routine technique though computational approach fails to give correct estimations of β values for structurally different systems and also for different reaction fields.[24, 40] The goal of this study, however, was not to obtain the exact values, but rather to estimate trends of β. It was reinforced by theoretical calculations and optical characterizations that the β value has a close relationship with the substituents, steric hindrance, and intramolecular charge-transfer. In order to model the ground state molecular geometries, the HOMO-LUMO energy gaps and first-order hyperpolarizability (β) of the chromophores, the DFT calculations were carried out at the PBE1PBE level by employing the split valence 6-31 g (d) basis set.[41-44] The data obtained from DFT calculations are summarized in Table.2.

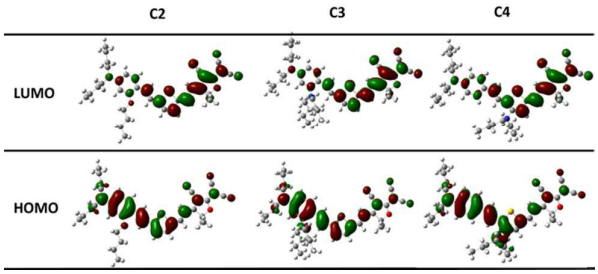

Fig 4. Frontier molecular orbitals of chromophores **C2**-**C4**

Table 2. Data from DFT calculations

	μ^a/D	ΔE^b/eV	$\mu\beta^c/10^{-48}$esu	$\beta^d_{zzz}/10^{-30}$esu
C1	20.06	2.32	11334	714.56
C2	22.74	2.29	16623	731.03
C3	21.59	2.26	16260	753.17
C4	21.38	2.17	16940	792.33

$^b\Delta E = E_{LUMO} - E_{HOMO}$. $^a\mu$, $^b\Delta E$, $^c\mu\beta_{zzz}$ and $^d\beta_{zzz}$ was calculated using Gaussian 09 at PBE1PBE/6-31g* level.

From this, the scalar quantity of β can be computed from the x, y, and z components according following equation.

$$\beta = (\beta_x^2 + \beta_y^2 + \beta_z^2)^{1/2}$$

Where

$$\beta_i = \beta_{iii} + \frac{1}{3}\sum_{i \neq j}(\beta_{ijj} + \beta_{jij} + \beta_{jji}), \quad i, j \in (x, y, z)$$

The frontier molecular orbitals are often used to characterize the chemical reactivity and kinetic stability of a molecule, and to obtain qualitative information about the optical and electrical properties of molecules.[24, 42] Besides, the HOMO-LUMO energy gap is also used to understand the charge transfer interaction occurring in a chromophore molecule.[45, 46] Fig.4 depicts the electron density distribution of the HOMO and LUMO structures. It can be seen that the density of the ground and excited state electron is asymmetry along the dipolar axis of the chromophores. The HOMO-LUMO gap was the lowest for **C4** (1.86 eV), highest for **C1** (2.32 eV). It proved that the same amino groups can show different effects in HOMO-LUMO energy gap and UV-Vis absorption when compared with **C3**. Introducing electron-donating group into 4-site of thiophene-bridge can effectively make the maximum absorption wavelength red-shift, narrow HOMO-LUMO energy gap and improve chromophore's first-order hyperpolarizability.

2.4 Crystal structure studies

It is an arduous task to grow single crystals for complicated molecules, particularly there are several flexible groups. After

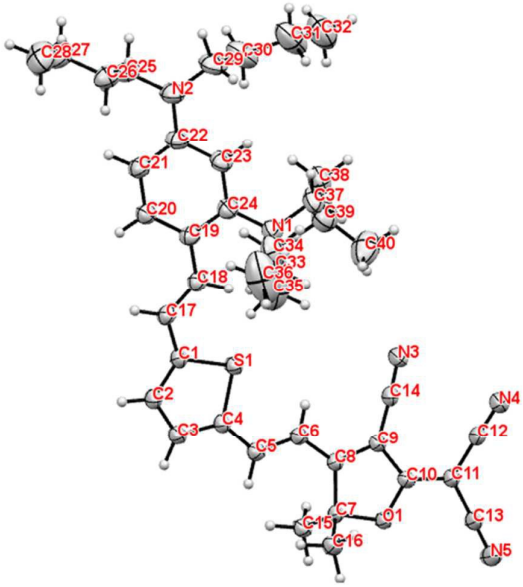

Fig 5. Thermal ellipsoid plot of **C3** drawn at the 30% level.

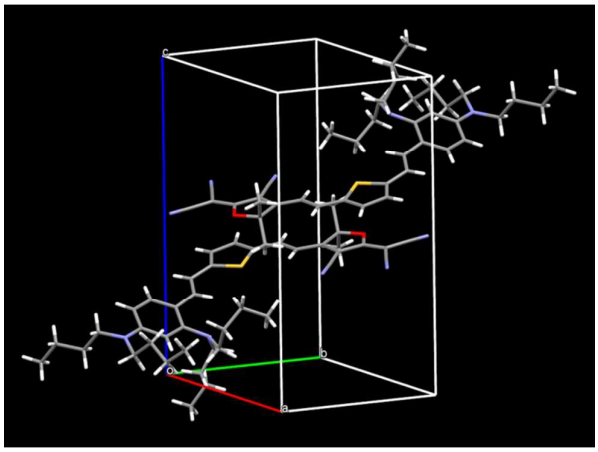

Fig 6. Crystal packing diagram of chromophore **C3**.

Table 4. Crystal data and structure refinement details for **C3**.

Compound reference	**C3**
Chemical formula	$C_{40}H_{51}N_5OS$
Formula mass	649.93
Crystal system	Triclinic
Wavelength/ Å	0.71073
a/Å	10.387(2)
b/Å	10.780(2)
c/Å	17.168(4)
α(°)	90.321(4)
β(°)	95.987(4)

γ(°)	93.823(4)
Calculated density/(g/ cm^3)	1.132
Unit cell volume/ $Å^3$	1907.4(7)
T/K	153
Space group	P-1
No. of formula units per units cell, Z	2
F(000)	700
No. of measured reflections	23561
No. of independent reflections	8813
R_{int}	0.035
Final R_1 values (I>2σ(I))	0.0598
Final wR(F^2)values (I>2σ(I))	0.1714
Goodness of fit on F^2	1.002

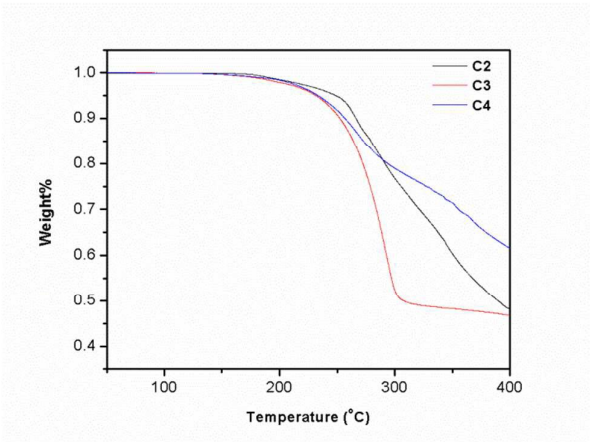

Fig.7 Thermogravimetric analysis of the chromophores **C2**- **C4**

several attempts, we successfully got eligible single crystal of **C3** by evaporation of ethanol/hexane solutions at ambient temperature. The ORTEP diagram and the crystal data are given in Fig 5 and Table 4 and crystal packing diagrams are shown in Fig 6. C3 crystallized in the triclinic space group P1. As Fig 5 shows, the molecular conformation, including the hindrance of donor and acceptor effectively isolates the chromophores and weakens the dipole– dipole interactions. This arrangement acts to site-isolate the chromophore within the internal free volume created by the butyl groups, which is favorable for dipole orientation in the poling process. The crystal packing data showed ring centroid to ring-centroid separations of 4.35 Å to 5.86 Å, which indicates better site isolation than that of the 4.2 Å reported previously.[44, 45] Although it was difficult to observe the H-bonding effects on proton shifts in the ^{1}H NMR spectrum of **C3**, efficient charge transfer in the trans conformation and the strong electron-

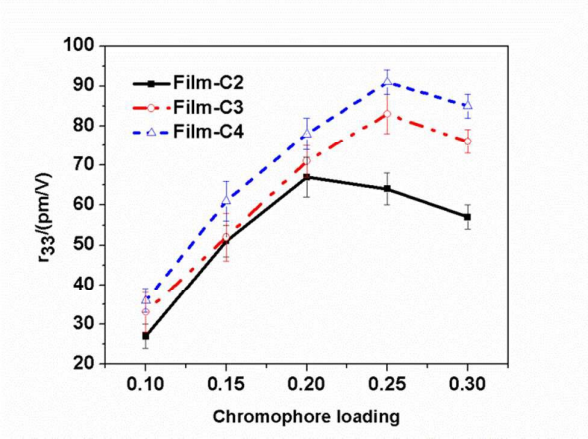

Fig 8. EO activities of thin films as a function of chromophore loading densities.

withdrawing effect of the TCF acceptor was shown by the crystal analytical data, which also showed intramolecular H-bonding interactions between C(6)--H(6)..S(1); C(18)--H(18)..S(1); C(18)--H(18)..N(1) (Fig 6) with a distance of 3.107 Å, 3.094 Å and 2.824 Å and an angle of 110°, 111° and 102°. Thus, it firmly supported the conclusion in the synthetic analysis that an intramolecular H-bonding interaction between indeed existed in **C3**.

2.3 Thermal stabilities and EO performance.

NLO chromophores must be thermally stable enough to withstand encountered high temperatures (>100°C) in electric field poling and subsequent processing of chromophore/polymer materials. Fig. 7 shows the thermogravimetric analysis of **C2**-**C4**. All of the chromophores exhibited good thermal stabilities and the decomposition temperatures (T_d) beyond 200 °C (**C2**: 246 °C, **C3**: 231 °C, **C4**: 233 °C). The temperature in practical materials processing was generally below 200°C. All of the chromophores **C2**-**C4** are highly stable and may be widely applied in photonic device fabrications.

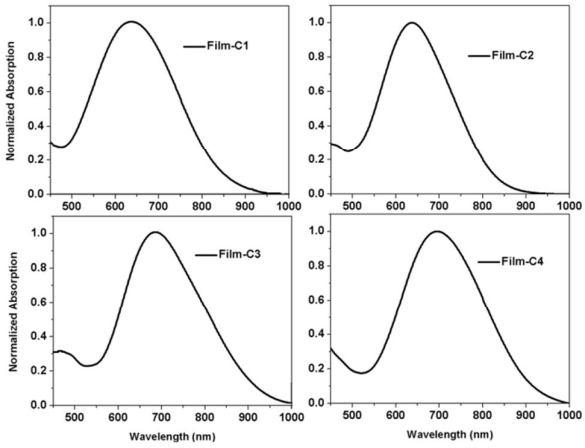

Fig. 9 UV-Vis spectra for film-**C1**, film-**C2**, film-**C3** and film-**C4**.

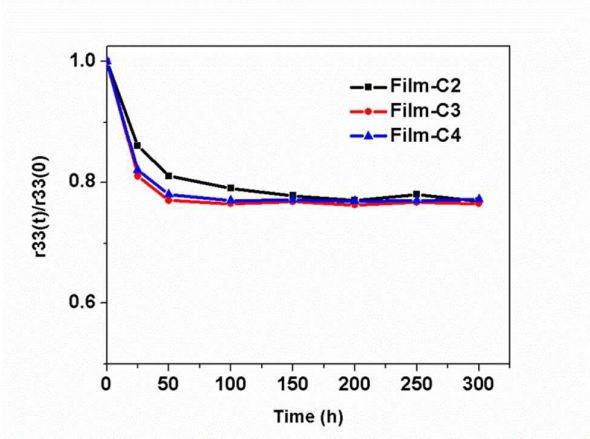

Fig 10. Temporal stabilities of the poled film-**C2**, film-**C3** and film-**C4** at 85 °C for 300h.

In order to evaluate their EO activities, the polymer films doped with 5wt%-30wt% chromophores into amorphous polycarbonate (APC) using 1,1,2-trichloroethane (TCE) as the solvent were prepared to investigate the translating of the microscopic hyperpolarizability into macroscopic EO response (r_{33}). The solution was filtered using a 0.2-μm syringe filter to remove large particulates. And then the solution was spin-coated on indium-tin oxide (ITO) glass substrates. The films were dried in vacuo for 12 h to remove the residual solvent. The thickness of the films was measured with an Ambios Technology XP-1 profilometer. The thickness of Guest-Host polymer films were about 2.1μm-2.6μm, which should be thicker than the films poled in contact poling to prevent the possible film damage (in contact poling, films thickness will be about 1.3μm-2.0μm). Chromophore's aggregation will not only diminish poling-induced noncentrosymmetric alignment of the chromophores, but also increase optical loss. Therefore, it was important to evaluate the molecular aggregation in guest-host films. Chromophore's aggregation generally will broaden the main CT peak. Before corona poling, we measured the UV-Vis spectra for four guest-host thin films doped with **C1-4** and shown in fig 9. Four films exhibited similar CT absorption peaks in different wavelengths. Film-**C1** showed s little bit broader than other three kinds of films, which indicated more severe chromophore's aggregation in film-**C1**.

The EO activities (r_{33} values) of poled films were measured by the Teng-Man simple reflection method at a wavelength of 1310 nm using a carefully selected thin ITO electrode with low reflectivity and good transparency in order to minimize the contribution from multiple reflections.[28, 47] Through changing the poling temperature, poling time and poling voltage, the optimum poling condition were poled at (T_g+5) °C for 15 min under the electric field of 10-11kV. The r_{33} values were measured and showed in Table 1 and Fig 7. **C2-C4** displayed excellent compatibility with polymer matrix when prepared guest-host polymers. Film-**C2**, Film-**C3** and Film-**C4** showed larger EO activities than Film-**C1**, which caused by higher first-order hyperpolarizabilities, larger steric hindrance and excellent compatibility with polymer matrix. With the increase of chromophore loading density, the EO activity of film-**C2** stopped growth at the soonest because of the gradually increased intermolecular interactions. Film-**C3** and film-**C4** showed saturated density and better EO activities in 25%wt higher than film-**C2**. The long-chain on the donor or bridge part, acting as the isolation group, may reduce inter-molecular electrostatic interactions, thus the molecular first-order hyperpolarizabilities can be more effectively translated into the macroscopic EO activity. After 300h at 75 °C, the EO activities can be retained above 75% of initial data. The $r_{33}(0)$ values were determined after poling. The r_{33} values of film **C3** and **C4** are two times higher than that of the traditional chromophore **C1** (39 pm/V)[48] suggested that by introducing heteroatom to the to the donor and bridge of conventional molecular can significantly increase their macroscopic EO activities.

3. Experimental

3. 1. General procedures.

All chemicals are commercially available and are used without further purification unless otherwise stated. N, N-dimethyl formamide (DMF) was distilled over calcium hydride and stored over molecular sieves (pore size 3Å). Acetone was dried with anhydrous MgSO4, then distilled and stored over molecular sieves (pore size 3Å). The 2-dicyanomethylene-3-cyano-4-methyl-2,5-dihydrofuran(TCF) acceptor was prepared according to the literature [21]. Compound 7c was prepared according to the literature []. TLC analyses were carried out on 0.25 mm thick precoated silica plates and spots were visualized under UV light. Chromatography on silica gel was carried out on Kieselgel (200-300 mesh). ^{1}H and ^{13}C NMR spectra were determined by Advance Bruker 400M (400 MHZ) NMR spectrometer (tetramethylsilane as internalreference). The MS spectra were obtained on MALDI-TOF (Matrix Assisted Laser Desorption/Ionization of Flight) on BIFLEXIII (Broker Inc.) spectrometer. The UV-Vis experiments were performed on Cary 5000 photo spectrometer. The TGA was determined by TA5000-2950TGA (TA co) with a heating rate of 10 °C min-1 under the protection of nitrogen. The single-crystal X-ray diffraction data were collected with the use of graphite-monochromatized Mo-Kα" radiation (λ=0.71073 Å) at -120 °C on a Rigaku AFC10 diffractometer equipped with a Saturn CCD detector.

3. 2. Synthesis

3. 2. 1. Compound 6a

To a stirred solution of aminophenol (1.09 g, 10mmol) and bromobutane (1.63 g, 15mmol) in 10mL DMF. Potassium carbonate (2.07 g, 15mmol) and 18-crown-6 (0.05 g, 0.2 mmol) were added. The reaction mixture was heated at 90 °C under nitrogen for 24h, then poured into 100mL solution of potassium carbonate. The reaction mixture was extracted by ethyl acetate (50mL×3), washed with brine, dried over $MgSO_4$. The solvent was removed in vacuo. The resulting crude product was purified by column chromatography with hexane/ethyl acetate as solvent, eluting with (V_{AcOEt}:V_{Hexane}=1:20) to give **6a** as pale oil with 84 % yield. ^{1}H NMR (400 MHz, $CDCl_3$, ppm): 7.09 (t, 1H, Ar-H), 6.27 (d, 1H, Ar-H), 6.19 (d, 2H, Ar-H), 3.95 (t, 2H, OCH_2), 3.24 (t, 4H, NCH_2), 1.76 (m, 2H, CH_2), 1.57 (m, 4H, CH_2), 1.49 (m, 2H, CH_2), 1.34 (m,

4H, CH_2), 0.96 (m, 9H, CH_3). ^{13}C NMR (101 MHz, $CDCl_3$, ppm): 189.35, 157.35, 153.00, 131.28, 106.43, 102.90, 54.95, 50.91, 29.68, 29.52, 20.49, 20.34, 13.92. MALDI-TOF (M+, $C_{18}H_{31}NO$): calcd: 277.24; found: 277.21.

3. 2. 2. Compound 6b

The procedure for compound **6a** was followed to prepare 6b from m-Phenylenediamine as colorless oil (91%). ^1H NMR (400 MHz, $CDCl_3$, ppm) δ=7.02 (t, J = 8.2 Hz, 1H, Ar-H), 6.00 (dd, J = 8.2, 2.1 Hz, 2H, Ar-H), 5.91 (d, J = 2.1 Hz, 1H, Ar-H), 3.35 – 3.18 (t, 8H, NCH_2), 1.58 (m, 8H, CH_2), 1.48 – 1.25 (m, 8H, CH_2), 1.08 – 0.90 (m, 12H, CH_3). ^{13}C NMR (101 MHz, $CDCl_3$, ppm): 150.14, 130.49, 101.02, 96.40, 51.97, 30.65, 21.33, 14.91. MALDI-TOF (M+, $C_{22}H_{40}N_2$): calcd: 332.22; found: 332.31.

3. 2. 3. Compound 7a

A solution of 20 mL DMF was cooled to 0 ºC and was maintained at this temperature during the dropwise addition of phosphorus oxychloride (0.64 g, 4.2mmol). The solution was kept stirring at 0 ºC for 2 h and the temperature was kept constant during the dropwise addition of **6a** (0.55g, 2mmol) in 10 mL DMF. The solution was stirred for 2h at 0 ºC, then gradually warmed to room temperature and stirred for 3 h at 60 ºC before being poured into 300 ml solution of potassium carbonate (10%) for quenching. The reaction mixture was extracted by ethyl acetate (50mL×3), washed with brine, dried over $MgSO_4$. After removing the solvent, the resulting crude product was purified by column chromatography with hexane/ethyl acetate (V_{AcOEt}:V_{Hexane}=1:8) as eluent to give the product as yellow oil (0.54g, 89%). ^1H NMR (400 MHz, $CDCl_3$): 10.15 (s, 1H, CHO), 7.67 (d, J = 8.9 Hz, 1H, Ar-H), 6.22 (d, J = 8.9 Hz, 1H, Ar-H), 5.98 (s, 1H, Ar-H), 4.00 (t, J = 6.3 Hz, 2H, OCH_2), 3.34 – 3.26 (t, 4H, NCH_2), 1.86 – 1.74 (m, 2H, CH_2), 1.68 – 1.54 (m, 4H, CH_2), 1.50 (m, 2H, CH_2), 1.44 – 1.30 (m, 4H, CH_2), 1.01 – 0.83 (m, 9H, CH_3). ^{13}C NMR (101 MHz, $CDCl_3$, ppm): 185.92, 162.79, 153.32, 129.02, 113.63, 103.54, 92.82, 66.87, 66.66, 49.92, 30.28, 29.79, 28.54, 19.28, 18.36, 17.94, 12.86, 12.75, 12.59. MALDI-TOF (M+, $C_{19}H_{31}NO_2$): calcd: 305.23; found: 305.22.

3. 2. 4. Compound 7b

The procedure for compound **7b** was followed to prepare **7a** from **6a** as yellow oil (V_{AcOEt}: V_{Hexane} = 1:8, 90%). ^1H NMR (400 MHz, $CDCl_3$, ppm): 10.05 (s, 1H, CHO), 7.70 (d, J = 8.9 Hz, Ar-H, CH), 6.32 (dd, J = 8.9, 2.3 Hz, 1H, Ar-H), 6.19 (d, J = 2.3 Hz, 1H, CH), 3.33 – 3.27 (t, 4H, NCH_2), 3.12 – 3.06 (t, 4H, NCH_2), 1.59 (m, 4H, CH_2), 1.49 (m, 4H, CH_2), 1.37 (m, 4H, CH_2), 1.26 (m, 4H, CH_2), 0.96 (t, 6H, CH_3), 0.87 (t, 6H, CH_3). ^{13}C NMR (101 MHz, Acetone) δ=205.91 (s), 188.57 (s), 157.20 (s), 153.23 (s), 131.30 (s), 120.84 (s), 107.26 (s), 103.82 (s), 49.22 (s), 45.07 (s), 12.87 (s), 12.64 (s). MALDI-TOF (M+, $C_{23}H_{40}N_2O$): calcd: 360.31; found: 360.31.

3. 2. 5. Compound 7c

A solution of 20 mL DMF and compound **6c** (0.42g, 2mmol) was cooled to 0 ºC and was maintained at this temperature during the dropwise addition of phosphorus oxychloride (0.34 g, 2.2mmol). The solution was stirred for 2h at 0 ºC, then gradually warmed to room temperature and stirred overnight before being poured into 300 ml solution of potassium carbonate (10%) for quenching. The reaction mixture was extracted by ethyl acetate (50mL×3), washed with brine, dried over $MgSO_4$. After removing the solvent, the resulting crude product was purified by column chromatography with hexane/ethyl acetate (V_{AcOEt}:V_{Hexane}=1:10) as eluent to give the product as pale oil (0.35g, 73%). ^1H NMR (400 MHz, $CDCl_3$) δ=9.70 (s, 1H, CHO), 7.48 (d, J = 5.6Hz, 1H, CH), 6.59 (d, J = 5.6 Hz, 1H, CH), 3.41 – 3.34 (m, 4H, NCH_2), 1.62 (m, 4H, CH_2), 1.33 (m, 4H, CH_2), 0.93 (t, 6H, CH_3). ^{13}C NMR (101 MHz, $CDCl_3$) δ=179.55, 153.84, 135.62, 119.86, 117.30, 54.29, 29.08, 19.75, 13.64. MALDI-TOF (M+, $C_{13}H_{21}NOS$): calcd: 239.13; found: 239.20.

3. 2. 6. Compound 8a

To a solution of compound **7a** (0.305g, 1 mmol) and 2-thienyl triphenylphosphonate bromide (0.48g, 1.1 mmol) in ether (20 ml) was added NaH (0.24g, 100 mmol). The solution was allowed to stir for 24h and then poured into water. The organic phase was extracted by AcOEt, washed with brine and dried over $MgSO_4$. After removal of the solvent under reduced pressure, the crude product was purified by silica chromatography, eluting with (V_{AcOEt}: V_{Hexane} = 1:20) to give compound **8a** as an orange oil (0.32 g, 83%). ^1H NMR (400 MHz, $CDCl_3$, ppm): 7.33 (d, J = 8.6 Hz, 1H, CH), 7.18 (d, J = 16.1 Hz, 1H, CH), 7.11 (d, J = 6.9 Hz, 1H, Ar-H), 7.07 (d, J = 4.9 Hz, 1H, CH), 6.95 (d, J=16.1 Hz, 1H, CH), 6.94 (s, 1H, CH), 6.24 (d, J = 6.9 Hz, 1H, Ar-H), 6.14 (s, 1H, Ar-H), 3.99 (t, 2H, OCH_2), 3.32–3.23 (m, 4H, NCH_2), 1.89–1.79 (m, 2H, CH_2), 1.57 (m, 6H, CH_2), 1.42 – 1.29 (m, 4H, CH_2), 1.01 (t, 3H, CH_3), 0.95 (t, 6H, CH_3). 13C NMR (101 MHz, $CDCl_3$, ppm): 156.92, 148.10, 144.18, 126.78, 126.33, 123.53, 122.68, 121.34, 116.45, 103.77, 95.51, 67.14, 49.91, 30.55, 28.67, 19.37, 18.49, 12.93, 12.88. MALDI-TOF (M+, $C_{24}H_{35}NOS$): calcd: 385.24; found: 385.24.

3. 2. 7. Compound 8b

The procedure for compound 8b was followed to prepare **8a** from **7a** as yellow solids (V_{AcOEt}: V_{Hexane} = 1:20, 72%). ^1H NMR (400 MHz, $CDCl_3$, ppm) δ 7.43 (d, J = 16.3 Hz, 1H, CH), 7.33 (d, J = 16.3 Hz, 1H, CH), 7.08 (t, J = 4.4 Hz, 1H, CH), 6.99 (d, J = 8.0 Hz, 1H, Ar-H), 6.96 (s, 1H, CH), 6.93 (d, J = 4.4 Hz, 1H, CH), 6.38 (d, J = 8.0 Hz, 1H, Ar-H), 6.35 (s, 1H, Ar-H), 3.30 – 3.24 (m, 4H, NCH_2), 2.99 – 2.93 (m, 4H, NCH_2), 1.63 – 1.54 (m, 4H, CH_2), 1.48 (m, 4H, CH_2), 1.36 (m, 4H, CH_2), 1.34 – 1.26 (m, 4H, CH_2), 1.00 – 0.94 (t, 6H, CH_3), 0.92 – 0.85 (t, 6H, CH_3). ^{13}C NMR (101 MHz, $CDCl_3$): 151.79, 148.67, 145.47, 142.44, 133.89, 131.48, 128.51, 125.91, 124.28, 121.55, 118.88, 107.61, 105.57, 104.04, 54.13, 53.30, 50.99, 29.88, 20.52, 14.01. MALDI-TOF (M+, $C_{28}H_{44}N_2S$): calcd: 440.32; found: 440.37.

3. 2. 8. Compound 8c

The procedure for compound 8c was followed to prepare **8a** from **7a** as yellow oil (V_{AcOEt}: V_{Hexane} = 1:20, 68%). ^1H NMR (400 MHz, $CDCl_3$) δ=7.25 (d, J = 8.6 Hz, 2H, Ar-H), 7.14 – 7.07 (d, J=16.3, 1H, CH), 6.89 (d, J = 5.3 Hz, 1H, CH), 6.80 (d, J = 5.3 Hz, 1H, CH), 6.67 (d, J = 16.3 Hz, 1H, CH), 6.53 (d, J = 8.6 Hz, 2H, Ar-H), 3.22 – 3.16 (m, 4H, CH_2), 2.86 – 2.78 (m, 4H, CH_2), 1.55 – 1.42 (m, 4H, CH_2), 1.36 – 1.17 (m, 12H, CH_2), 0.87 (t, 6H, CH_3),

0.78 (t, 6H, CH_3). ^{13}C NMR (101 MHz, CDCl3) δ=146.75, 131.97, 128.69, 126.36, 125.41, 124.32, 122.21, 119.81, 115.38, 110.91, 54.68, 49.85, 29.15, 28.59, 19.45, 19.37, 12.96. MALDI-TOF (M+, **C2**8H44N2S): calcd: 440.32; found: 440.37.

3. 2. 9. Compound 9a

To a solution of compound **8a**(0.77g, 2 mmol) in dry THF (30 mL), butyllithium (1.00 mL, 2.4 mmol, 2.4 M in hexane) was added dropwise at-78 °C. The mixture was stirred at -78 °C for 1h, then allowed to slowly warm to-20 °C for 10 min. After the mixture was cooled back down to-78 °C, 1.00 mL of DMF was added dropwise. The mixture was then slowly warmed to room temperature and stirred for 2h at room temperature; 30 mL of water was added to quench the reaction. After the solvent was evaporated, the organic layer was extracted with ethyl ether (3x50 mL). The combined organic layers were washed with water (50 mL) and brine (50 mL) and dried over anhydrous $MgSO_4$. After removal of the solvent under reduced pressure, the crude product was purified by silica chromatography, eluting with (V_{AcOEt}: V_{Hexane} = 1:8) to give compound **9a** as an orange oil (0.73 g, 88%). ^{1}H NMR (400 MHz, $CDCl_3$) δ=9.69 (s, 1H, CHO), 7.51 (d, J = 3.7 Hz, 1H, CH), 7.34 (d, J = 16.1 Hz, 1H, CH), 7.24 (s, 1H, CH), 7.03 – 6.96 (d, J=16.1 Hz, 1H, CH), 6.90 (d, J = 3.7 Hz, 1H, Ar-H), 6.19 (d, J = 1.5Hz, 1H, Ar-H), 6.03 (d, J = 1.5 Hz, 1H, Ar-H), 3.92 (t, 2H, OCH_2), 3.26 – 3.16 (t, 4H, CH_2), 1.81 – 1.73 (m, 2H, CH_2), 1.50 (m , 4H, CH_2), 1.37 – 1.24 (m, 2H, CH_2), 1.24 – 1.13 (m, 4H, CH_2), 0.94 (t , 4H, CH_2), 0.88 (t, 6H, CH_3). ^{13}C NMR (101 MHz, $CDCl_3$) δ=182.06, 158.86, 155.96, 137.53, 129.55, 128.81, 124.28, 116.05, 104.93, 95.94, 50.92, 39.14, 29.70, 25.77, 23.40, 20.39, 14.10, 13.93. MALDI-TOF (M+, $C_{25}H_{35}NO_2S$): calcd: 413.24; found: 413.21.

3. 2. 10. Compound 9b

The procedure for compound **9b** was followed to prepare **9a** from **8a** as orange oil (V_{AcOEt}: V_{Hexane} = 1:8, 75%). ^{1}H NMR (400 MHz, $CDCl_3$) δ=9.80 (s, 1H, CHO), 7.63 (d, J = 6.7 Hz, 1H, CH), 7.60 (d, J = 6.7 Hz, 1H, CH), 7.45 (d, J = 16.2 Hz, 1H, CH), 7.00 (d, J = 8.8 Hz, 1H, Ar-H), 6.95 (d, J = 16.2 Hz, 1H, CH), 6.38 (dd, J = 8.8, 2.5 Hz, 1H, Ar-H), 6.33 (d, J = 2.5 Hz, 1H, Ar-H), 3.32 – 3.25 (m, 4H, CH_2), 2.99 – 2.92 (m, 4H, CH_2), 1.63 – 1.53 (m, 4H, CH_2), 1.47 (m, 4H, CH_2), 1.37 (m, 4H, CH_2), 1.28 (m, 4H, CH_2), 0.97 (t, 6H, CH_3), 0.87 (t, 6H, CH_3). ^{13}C NMR (101 MHz, $CDCl_3$) δ=181.20, 155.11, 151.49, 148.16, 138.58, 138.58, 136.71, 130.74, 126.50, 123.34, 118.50, 113.90, 106.37, 103.97, 53.11, 49.85, 28.52, 19.91, 12.96. MALDI-TOF (M+, $C_{29}H_{44}N_2OS$): calcd: 468.32; found: 468.22.

3. 2. 11. Compound 9c

The procedure for compound **9c** was followed to prepare **9a** from **8a** as orange oil (V_{AcOEt}: V_{Hexane} = 1:8, 73%). ^{1}H NMR (400 MHz, $CDCl_3$) δ 9.63 (s, 1H, CHO), 7.45 (s, 1H, CH), 7.25 (d, J = 8.6 Hz, 2H, Ar-H), 7.08 (d, J = 16.2 Hz, 1H, CH), 6.91 (d, J = 16.2 Hz, 1H, CH), 6.50 (d, J = 8.6 Hz, 2H, Ar-H), 3.23 – 3.11 (m, 4H, NCH2), 2.83 (t, J = 7.2 Hz, 4H, NCH_2), 1.51 – 1.40 (m, 4H, CH_2), 1.36 – 1.27 (m, 4H, CH_2), 1.27 – 1.14 (m, 8H, CH_2), 0.84 (t, 6H, CH_3), 0.77 (t, 6H, CH_3). ^{13}C NMR (101 MHz, $CDCl_3$) δ=180.77, 147.70, 147.48, 143.45, 135.95, 131.36, 130.39, 127.28, 122.92, 113.76, 110.55, 54.24, 49.76, 28.97, 28.52, 19.40, 19.33, 12.95. MALDI-TOF (M+, $C_{29}H_{44}N_2OS$): calcd: 468.32; found: 468.30.

3. 2. 12. Chromophore 2

Compound **9a** (0.41 g, 1.00 mmol) and TCF acceptor (0.22 g, 1.10mmol) were dissolved in the anhydrous ethanol. The reaction mixture was allowed to stir at 60 °C for 1–3 h and monitored by TLC. After removal of the solvents, the residue was purified by column chromatography eluting with hexane/ethyl acetate. The desired chromophore was dark blue powder. (V_{AcOEt}: V_{Hexane} = 1:5, 0.32 g, yield: 54%). ^{1}H NMR δ=8.00 (d, J = 15.7 Hz, 1H, CH), 7.53 (d, J = 4.0 Hz, 1H, CH), 7.33 (dd, J = 12.4, 9.1 Hz, 2H, CH), 7.17 (d, J = 9.1 Hz, 1H, Ar-H), 7.01 (d, J = 4.0 Hz, 1H, CH), 6.65 (d, J = 15.7 Hz, 1H, CH), 6.23 (dd, J = 9.1, 2.1 Hz, 1H, Ar-H), 6.14 (d, J = 2.1 Hz, 1H, Ar-H), 4.00 (d, J = 6.4 Hz, 2H, CH_2), 3.27 (d, J = 7.5 Hz, 4H, CH_2), 2.66 (d, J = 6.4 Hz, 2H, CH_2), 1.75 (s, 6H, CH_3), 1.50–1.44 (m, 4H, CH_2), 1.32 – 1.20 (m, 4H, CH_2), 0.90 (t, 3H, CH_3), 0.84 (t, 6H, CH_3).

^{13}C NMR (101 MHz, Acetone) δ 176.06 (s), 173.71, 158.60, 154.75, 150.14, 139.34, 137.78, 136.79, 129.64, 128.84, 126.17, 115.38, 112.03, 111.27, 110.47, 104.42, 97.46, 95.94, 94.89, 67.17, 49.91, 30.73, 24.91, 19.46, 18.80, 12.84. MALDI-TOF, m/z: 594.31.

HRMS (ESI) (M+, $C_{40}H_{51}N_5OS$): calcd: 594.30285; found: 594.30291.found: 594.30287.

3. 2. 12. Chromophore C3

The procedure for chromophore **C3** was followed to prepare chromophore **C2** from 9a as dark powder (48%). ^{1}H NMR (400 MHz, $CDCl_3$) δ=7.77 (d, J = 15.5 Hz, 1H, CH), 7.62 (d, J = 16.0 Hz, 1H, CH), 7.47 (d, J = 8.7 Hz, 1H, Ar-H), 7.38 (d, J = 3.7 Hz, 1H, CH), 7.01 (s, 1H, Ar-H), 6.98 (d, J = 16.0 Hz, 1H, CH), 6.53 (d, J = 15.5 Hz, 1H, CH), 6.39 (d, J = 8.7 Hz, 1H, Ar-H), 6.33 (d, J=3.7Hz, 1H, CH), 3.39 – 3.24 (m, 4H, NCH_2), 3.08 – 2.94 (m, 4H, NCH_2), 1.75 (s, 6H, CH_3), 1.60 (m, 4H, CH_2), 1.54 – 1.45 (m, 4H, CH_2), 1.43 – 1.24 (m, 12H, CH_2), 0.97 (t, 6H, CH_3), 0.89 (t, 6H, CH_3).

^{13}C NMR (101 MHz, Acetone) δ=178.14, 176.07, 158.00, 154.21, 147.13, 132.53, 118.64, 114.08, 113.34, 112.96, 109.77, 107.53, 105.51, 97.74, 90.98, 54.69, 51.41, 26.56, 20.96, 20.66, 14.06. MALDI-TOF, m/z: 649.35.

HRMS (ESI) (M+, $C_{40}H_{51}N_5OS$): calcd: 649.38143; found: 649.38121.

3. 2. 13. Chromophore C4

The procedure for chromophore **C4** was followed to prepare chromophore **C2** from **9a** as dark powder (61%). ^{1}H NMR (400 MHz, $CDCl_3$) δ=7.69 (d, J = 15.7 Hz, 1H, CH), 7.31 (d, J = 8.3 Hz, 2H, Ar-H), 7.21 (s, 1H, CH), 7.09 (d, J = 15.1 Hz, 1H, CH), 6.94 (d, J = 15.7 Hz, 1H, CH), 6.56 (d, J = 8.3 Hz, 2H, Ar-H), 6.44 (d, J = 15.1 Hz, 1H, CH), 3.24 (t, 4H, CH_2), 2.90 (t, 4H, CH_2), 1.65 (m, 4H, CH_2), 1.57 – 1.45 (m, 4H, CH_2), 1.41 – 1.18 (m, 8H, CH_2), 0.89 (t, 6H, CH_3), 0.82 (t, 6H, CH_3). ^{13}C NMR (101 MHz, $CDCl_3$) δ=174.98, 171.61, 149.82, 147.99, 144.14, 138.28, 133.55, 132.22, 131.28, 127.79, 122.72, 113.45, 110.79, 109.56, 95.78, 53.84, 49.77, 29.73, 28.81, 28.51, 25.47, 19.28, 12.87.

HRMS (ESI) (M+, **C4**0H51N5OS): calcd: 649.38143; found: 649.38138.

Conclusions

three organic NLO chromophores modified by heteroatom group based on Dewar' Rules have been synthesized and systematically characterized by NMR, MS, UV-Vis absorption spectra, and single-crystal X-ray diffraction methods. The new compounds obtained good yields which are ensured by the simple work-up procedures. Thermogravimetric analysis showed good thermal and thermoxidative stabilities of the four chromophores. The effects of bathochromic and solvatochromic behavior on the UV-Vis absorption were also investigated to compare different electron donating abilities and polarizability. Meanwhile, DFT calculations were carried out to analyze the effects of different heteroatom matches on chromophores' first-order hyperpolarizabilities. The calculating data showed nice consistency with the analysis of UV-Vis spectra and electro-optical measurement. All of three chromophores showed good solubility and comparability with polymer which were crucial to make high quality EO devices. The doped polymer films containing chromophore **C2-4** displayed higher r_{33} values than Film-**C1** (the doping concentration of **C1** cannot exceed 20%) at the doping concentration of 25 wt% blended in APC. Film-**C4** exhibited the highest r_{33} value owing to efficiently enhanced microscopic optical nonlinear activity and steric hindrances in donor and bridge. All these might be useful in designing other new NLO chromophores with modified heteroatoms groups to optimize molecular structure for achieving high performance.

Acknowledgements

We are grateful to the Directional Program of the Chinese Academy of Sciences (KJCX2.YW.H02), Innovation Fund of Chinese Academy of Sciences (CXJJ-11-M035) and National Natural Science Foundation of China (No. 11104284 and No. 61101054) for the financial support.

References

1. F. Kajzar, K. S. Lee and A. K. Y. Jen, in *Polymers for Photonics Applications Ii: Nonlinear Optical, Photorefractive and Two-Photon Absorption Polymers*, ed. K. S. Lee, 2003, vol. 161, pp. 1-85.
2. C. Zhang, L. R. Dalton, M. C. Oh, H. Zhang and W. H. Steier, *Chem. Mater.*, 2001, **13**, 3043-3050.
3. H. Kang, A. Facchetti, P. W. Zhu, H. Jiang, Y. Yang, E. Cariati, S. Righetto, R. Ugo, C. Zuccaccia, A. Macchioni, C. L. Stern, Z. F. Liu, S. T. Ho and T. J. Marks, *Angewandte Chemie-International Edition*, 2005, **44**, 7922-7925.
4. M. Hochberg, T. Baehr-Jones, G. X. Wang, M. Shearn, K. Harvard, J. D. Luo, B. Q. Chen, Z. W. Shi, R. Lawson, P. Sullivan, A. K. Y. Jen, L. Dalton and A. Scherer, *Nat. Mater.*, 2006, **5**, 703-709.
5. T. D. Kim, J. W. Kang, J. D. Luo, S. H. Jang, J. W. Ka, N. Tucker, J. B. Benedict, L. R. Dalton, T. Gray, R. M. Overney, D. H. Park, W. N. Herman and A. K. Y. Jen, *J. Am. Chem. Soc.*, 2007, **129**, 488-489.
6. J. Y. Wu, S. H. Bo, J. L. Liu, T. T. Zhou, H. Y. Xiao, L. Qiu, Z. Zhen and X. H. Liu, *Chem. Commun.*, 2012, **48**, 9637-9639.
7. J. Liu, H. Xu, X. Liu, Z. Zhen, W. Kuznik and I. V. Kityk, *Journal of Materials Science: Materials in Electronics*, 2011, **23**, 1182-1187.
8. H. Huang, G. Deng, J. Liu, J. Wu, P. Si, H. Xu, S. Bo, L. Qiu, Z. Zhen and X. Liu, *Dyes Pigm.*, 2013, **99**, 753-758.
9. H. Xu, M. Zhang, A. Zhang, G. Deng, P. Si, H. Huang, C. Peng, M. Fu, J. Liu, L. Qiu, Z. Zhen, S. Bo and X. Liu, *Dyes Pigm.*, 2014, **102**, 142-149.
10. M. Lee, H. E. Katz, C. Erben, D. M. Gill, P. Gopalan, J. D. Heber and D. J. McGee, *Science*, 2002, **298**, 1401-1403.
11. L. R. Dalton, P. A. Sullivan and D. H. Bale, *Chem. Rev.*, 2010, **110**, 25-55.
12. J. Y. Wu, J. L. Liu, T. T. Zhou, S. H. Bo, L. Qiu, Z. Zhen and X. H. Liu, *Rsc Advances*, 2012, **2**, 1416-1423.
13. J. Liu, G. Xu, F. Liu, I. Kityk, X. Liu and Z. Zhen, *RSC Advances*, 2015, **5**, 15784-15794.
14. P. Si, J. Liu, Z. Zhen, X. Liu, G. Lakshminarayana and I. Kityk, *Tetrahedron Lett.*, 2012, **53**, 3393-3396.
15. J. Liu, H. Xu, X. Liu, Z. Zhen, W. Kuznik and I. Kityk, *Journal of Materials Science: Materials in Electronics*, 2012, **23**, 1182-1187.
16. S. R. Marder, B. Kippelen, A. K.-Y. Jen and N. Peyghambarian, *Nature*, 1997, **388**, 845-851.
17. S. Liu, M. A. Haller, H. Ma, L. R. Dalton, S. H. Jang and A. K. Y. Jen, *Adv. Mater.*, 2003, **15**, 603-607.
18. D. R. Kanis, M. A. Ratner and T. J. Marks, *Chem. Rev.*, 1994, **94**, 195-242.
19. M. J. Cho, D. H. Choi, P. A. Sullivan, A. J. P. Akelaitis and L. R. Dalton, *Prog. Polym. Sci.*, 2008, **33**, 1013-1058.
20. S. J. Benight, D. H. Bale, B. C. Olbricht and L. R. Dalton, *J. Mater. Chem.*, 2009, **19**, 7466-7475.
21. M. Q. He, T. M. Leslie and J. A. Sinicropi, *Chem. Mater.*, 2002, **14**, 4662-4668.
22. J. D. Luo, M. Haller, H. Ma, S. Liu, T. D. Kim, Y. Q. Tian, B. Q. Chen, S. H. Jang, L. R. Dalton and A. K. Y. Jen, *J. Phys. Chem. B*, 2004, **108**, 8523-8530.
23. B. C. Rinderspacher, J. Andzelm, A. Rawlett, J. Dougherty, D. N. Beratan and W. Yang, *J. Chem. Theory Comput.*, 2009, **5**, 3321-3329.
24. J. A. Davies, A. Elangovan, P. A. Sullivan, B. C. Olbricht, D. H. Bale, T. R. Ewy, C. M. Isborn, B. E. Eichinger, B. H. Robinson and P. J. Reid, *J. Am. Chem. Soc.*, 2008, **130**, 10565-10575.
25. Y.-J. Cheng, J. Luo, S. Huang, X. Zhou, Z. Shi, T.-D. Kim, D. H. Bale, S. Takahashi, A. Yick and B. M. Polishak, *Chem. Mater.*, 2008, **20**, 5047-5054.
26. C. Zhang, C. Wang, J. Yang, L. R. Dalton, G. Sun, H. Zhang and W. H. Steier, *Macromolecules*, 2001, **34**, 235-243.
27. J. M. Elward and B. C. Rinderspacher, *PCCP*, 2015.
28. O.-P. Kwon, M. Jazbinsek, H. Yun, J.-I. Seo, J.-Y. Seo, S.-J. Kwon, Y. S. Lee and P. Günter, *CrystEngComm*, 2009, **11**, 1541-1544.
29. T. Yamada, H. Miki, I. Aoki and A. Otomo, *Opt. Mater.*, 2013, **35**, 2194-2200.
30. M. Dewar, *Journal of the Chemical Society (Resumed)*, 1950, 2329-2334.
31. M. Blanchard‐Desce, V. Alain, P. Bedworth, S. Marder, A. Fort, C. Runser, M. Barzoukas, S. Lebus and R. Wortmann, *Chemistry-A European Journal*, 1997, **3**, 1091-1104.
32. J. Hung, W. Liang, J. Luo, Z. Shi, A. K.-Y. Jen and X. Li, *The Journal of Physical Chemistry C*, 2010, **114**, 22284-22288.

33. M. Q. He, T. M. Leslie and J. A. Sinicropi, *Chem. Mater.*, 2002, **14**, 2393-2400.
34. S. M. Budy, S. Suresh, B. K. Spraul and D. W. Smith, *J. Phys. Chem. C*, 2008, **112**, 8099-8104.
35. K. P. Guo, J. M. Hao, T. Zhang, F. H. Zu, J. F. Zhai, L. Qiu, Z. Zhen, X. H. Liu and Y. Q. Shen, *Dyes Pigm.*, 2008, **77**, 657-664.
36. B. K. Spraul, S. Suresh, T. Sassa, M. A. Herranz, L. Echegoyen, T. Wada, D. Perahia and D. W. Smith, *Tetrahedron Lett.*, 2004, **45**, 3253-3256.
37. Y. J. Cheng, J. D. Luo, S. Hau, D. H. Bale, T. D. Kim, Z. W. Shi, D. B. Lao, N. M. Tucker, Y. Q. Tian, L. R. Dalton, P. J. Reid and A. K. Y. Jen, *Chem. Mater.*, 2007, **19**, 1154-1163.
38. S. R. Marder, C. B. Gorman, B. G. Tiemann, J. W. Perry, G. Bourhill and K. Mansour, *Science*, 1993, **261**, 186-189.
39. F. Meyers, S. Marder, B. Pierce and J. Bredas, *J. Am. Chem. Soc.*, 1994, **116**, 10703-10714.
40. D. H. Bale, B. E. Eichinger, W. Liang, X. Li, L. R. Dalton, B. H. Robinson and P. J. Reid, *The Journal of Physical Chemistry B*, 2011, **115**, 3505-3513.
41. J. Andzelm, B. C. Rinderspacher, A. Rawlett, J. Dougherty, R. Baer and N. Govind, *J. Chem. Theory Comput.*, 2009, **5**, 2835-2846.
42. M. Frisch, G. Trucks, H. Schlegel, G. Scuseria, M. Robb, J. Cheeseman, J. Montgomery Jr, T. Vreven, K. Kudin and J. Burant, *Gaussian Inc., Pittsburgh, PA*, 2003.
43. C. Lee and R. G. Parr, *Physical Review A*, 1990, **42**, 193-200.
44. M. Frisch, G. Trucks, H. B. Schlegel, G. Scuseria, M. Robb, J. Cheeseman, G. Scalmani, V. Barone, B. Mennucci and G. Petersson, *Wallingford, CT*, 2009, **19**, 227-238.
45. R. V. Solomon, P. Veerapandian, S. A. Vedha and P. Venuvanalingam, *J. Phys. Chem. A*, 2012, **116**, 4667-4677.
46. R. M. El-Shishtawy, F. Borbone, Z. M. Al-Amshany, A. Tuzi, A. Barsella, A. M. Asiri and A. Roviello, *Dyes Pigm.*, 2013, **96**, 45-51.
47. J. Chiffre, F. Averseng, G. G. Balavoine, J. C. Daran, G. Iftime, P. G. Lacroix, E. Manoury and K. Nakatani, *Eur. J. Inorg. Chem.*, 2001, **2001**, 2221-2226.
48. Y. Yang, H. Xu, F. Liu, H. Wang, G. Deng, P. Si, H. Huang, S. Bo, J. Liu, L. Qiu, Z. Zhen and X. Liu, *Journal of Materials Chemistry C*, 2014, **2**, 5124-5132.